

# Hybrid schemes to compute contact discontinuities in Euler equations with any EOS

Thierry Gallouët<sup>a</sup>, Jean-Marc Hérard<sup>a,b</sup>, Nicolas Seguin<sup>a,b</sup>

<sup>a</sup> L.A.T.P. (UMR 6632), C.M.I., Université de Provence, 39, rue Joliot Curie, 13453 Marseille cedex 13, France

<sup>b</sup> Département M.F.T.T., E.D.F. recherche et développement, 6, quai Watier, 78401 Chatou cedex, France

Received 26 September 2001; accepted after revision 6 May 2002

Note presented by Michel Combarrous.

---

## Abstract

We propose here some explicit hybrid schemes which enable accurate computation of Euler equations with arbitrary (analytic or tabulated) equation of state (EOS). The method is valid for the exact Godunov scheme and some approximate Godunov schemes. *To cite this article: T. Gallouët et al., C. R. Mécanique 330 (2002) 445–450.* © 2002 Académie des sciences/Éditions scientifiques et médicales Elsevier SAS

computational fluid mechanics / Euler equations / Godunov schemes

## Schémas hybrides pour la simulation des discontinuités de contact des équations d'Euler avec une loi d'état quelconque

## Résumé

On propose un schéma explicite hybride permettant d'effectuer des simulations précises des équations d'Euler pour un choix de loi thermodynamique quelconque, analytique ou tabulée. La méthode est définie pour les schémas de Godunov exact ou approchés. *Pour citer cet article: T. Gallouët et al., C. R. Mécanique 330 (2002) 445–450.* © 2002 Académie des sciences/Éditions scientifiques et médicales Elsevier SAS

mécanique des fluides numérique / équations d'Euler / schémas de Godunov

---

## Version française abrégée

La simulation des écoulements diphasiques de type eau-vapeur, ou de certains écoulements monophasiques compressibles nécessite l'utilisation de lois d'état assez complexes, qui peuvent parfois même n'être que tabulées. Il en est de même pour la simulation des écoulements multi-matériaux dans certaines configurations. La représentation de ces phénomènes se fait couramment à l'aide des équations d'Euler (ou de modèles de type Navier–Stokes pour prendre en compte les effets de viscosité), ou de modèles plus complexes dits à deux fluides, qui nécessitent clairement une excellente maîtrise du système précédent. Or, lorsque la thermodynamique s'écarte du comportement de la loi des gaz parfaits monoconstituants, les schémas conservatifs utilisant une stabilisation par décentrement (par exemple le schéma de Godunov [1]) se comportent de manière médiocre au voisinage des discontinuités de contact (sans inhiber la convergence). De fortes oscillations peuvent apparaître, et dans la meilleure configuration, la vitesse de convergence très lente [13] (de type  $h^{1/2}$ ) interdit la prédiction précise de certains phénomènes physiques. Plusieurs auteurs ont proposé des méthodes permettant de contourner ces difficultés, en se focalisant essentiellement

---

*E-mail addresses:* Thierry.Gallouet@cmi.univ-mrs.fr (T. Gallouët); Herard@cmi.univ-mrs.fr, Jean-Marc.Herard@der.edf.fr (J.-M. Hérard); seguin@chi80bk.der.edf.fr (N. Seguin).

sur le mélange de gaz parfaits, ou de manière analogue sur la loi d'état « stiffened gas » [5–7]. Récemment, une contribution au débat concernant la loi d'état de Van der Waals a été proposée par Shyue [8]. Une approche distincte a été proposée dans [14]. On se propose ici de donner un cadre général permettant d'effectuer des simulations avec tout type de loi thermodynamique, en se focalisant sur le schéma de Godunov et sur une large classe de solveurs de Godunov approchés tels qu'introduits récemment [3,4], et utilisant la variable  $Y^t = (U, P, g(\rho, s), C, \psi)$  (les notations sont introduites dans la partie anglaise). Pour cela, il est tout d'abord nécessaire de décomposer l'énergie interne  $\rho e = E - \rho U^2/2$  en fonction des variables  $P, \rho, C, \psi$  (respectivement pression, densité, concentration et fonction couleur) sous la forme :  $\rho e = \phi_1(P, \rho, C, \psi) + f_2(C, \psi)h_2(P) + g_2(C, \psi) + \phi_3(P, \rho, C, \psi)$ . Les fonctions  $\phi_1$  sont de la forme :  $\phi_1(P, \rho, C, \psi) = \rho(a_1(P) + b_1(P)C + c_1(P)\psi) + d_1(P)$ . Pour traiter les situations où la loi d'état n'est pas dans  $T_1$ , on propose le schéma explicite modifié suivant (4) pour simuler le système conservatif hyperbolique non strict (1), où les grandeurs  $C$  et  $\psi$  sont « convectées » à la vitesse  $U$  (ce qui est crucial pour le traitement des lois dans  $T_2$ ). Ce schéma nécessite seulement de définir la pression de maille  $p_i^{n+1}$  en fin de pas de temps comme la solution  $\tilde{P}_i^{n+1}$  de l'équation de maille (5). Il permet de représenter parfaitement sur maillage « grossier » les discontinuités de contact instationnaires au sens suivant : *si la condition initiale discrète est telle que :  $U_k^n = U_0$  et  $p_k^n = P_0$  pour  $k = i - 1, i, i + 1$ , le schéma doit fournir des valeurs de pression et de vitesse de maille au pas de temps suivant telles que :  $p_i^{n+1} = P_0$  et  $U_i^{n+1} = U_0$* . On retrouve naturellement la proposition d'Abgrall et Saurel pour la loi « stiffened gas » caractéristique de la classe  $T_2$ . Le schéma est basé sur la discrétisation des équations redondantes (6) en zone régulière. La validation de ce schéma nécessite un examen précis du comportement de la suite d'approximations en présence de chocs, lorsque le pas de maillage tend vers 0, à nombre de CFL constant. Dans le cas d'une thermodynamique dans  $T_2$ , il est intéressant de constater que la vitesse de convergence (Fig. 2) mesurée en norme  $L^1$  est en tout point identique pour la variable densité à celle de la concentration [13]. De surcroît, la vitesse de convergence pour les variables  $U, P$  qui sont invariantes à travers le contact est de 1 (elle est de 1/2 dans le cas du schéma conservatif de base). Le schéma semble donc fournir une approximation convergeant vers la bonne solution, ce qui est cohérent avec la spécificité de la classe  $T_2$  [13]. Le comportement du schéma modifié est encore très bon sur maillage grossier, lorsque la loi d'état comporte une contribution dans  $T_3$  (Van der Waals, Chemkin, ...), mais la simulation numérique d'un « vrai » produit non conservatif perturbe la convergence sur maillage très fin (plus de  $10^4$  noeuds en dimension 1, voir Fig. 4, et également [9]). Ce résultat suggère ainsi d'utiliser le schéma modifié sur maillage grossier de préférence, et le dernier point est confirmé par une analyse de sensibilité à la décomposition thermodynamique [13].

La méthode se comporte bien pour les configurations thermodynamiques considérées, analytiques (loi « stiffened gas », loi de Van der Waals [10], Chemkin [11]) ou tabulées [12]. Pour les lois de type Chemkin ou les lois analytiques complexes, le coût calcul pour l'obtention de  $\tilde{P}_i^n$  solution de (5) est beaucoup plus faible en pratique que celui associé à  $P_i^n$  solution de  $e(P_i^n, \rho_i^n, C_i^n, \psi_i^n) = e_i^n$  (méthode classique) ; l'algorithme modifié est dès lors plus performant en terme de précision et de coût, à maillage donné. On renvoie le lecteur à [13] pour plus de détails. Les extensions à l'ordre deux par des techniques de type MUSCL sont possibles.

## 1. Introduction

We focus here on the computation of Euler equations with arbitrary type of equation of state (EOS) with help of exact Godunov scheme [1,2], or some particular approximate Godunov schemes issuing from VFRoe-ncv formalism with help of  $Y^t = (U, P, g(\rho, s), C, \psi)$  variables – see notations below –, [3,4]. The main objective here is to derive schemes which 'perfectly resolve unsteady contact discontinuities in Euler equations' in the following sense: *if the initial data is in agreement with:  $U_k^n = U_0$  and  $p_k^n = P_0$  with  $k = i - 1, i, i + 1$ , the scheme must provide updated cell pressures and cell velocities such that:  $p_i^{n+1} = P_0$ , and  $U_i^{n+1} = U_0$* . Some ways to deal with simple analytic laws have been suggested recently by several

authors (see [5–7] for stiffened gas EOS and mixture of perfect gases, [8] for Van der Waals EOS for instance). No general frame work clearly arises in order to deal with arbitrary state law. This is one objective of the present work, which also aims at clarifying the true rate of convergence achieved in some specific cases, and the achieved accuracy level on given mesh size. First, we introduce some classification of EOS based on three classes. Unsteady contact discontinuities are perfectly represented on coarse or fine meshes for EOS belonging to the first class. We then propose some generic way to account for any EOS using decomposition of the EOS on the three classes, and introducing some adequate scheme to deal with the whole. On the basis of several one dimensional Riemann problems, the  $L^1$  error norm is plotted which confirms the behaviour is rather good though it is not a fully conservative scheme (see [9]). Exact analytic EOS such as stiffened gas EOS, mixture of perfect gases, Van der Waals EOS [10] those arising in Chemkin database [11], or tabulated laws [12] may be used with the present approach. Details can be found in [13].

## 2. Governing equations and classification of EOS

The one-dimensional governing set of Euler equations takes the form ( $x$  in  $\mathbb{R}$ ):

$$\begin{cases} \frac{\partial W}{\partial t} + \frac{\partial F(W)}{\partial x} = 0, \\ W(x, 0) = W_0(x) \end{cases} \quad (1)$$

with  $W = (\rho, \rho C, \rho U, E, \rho \psi)$ ,  $F(W) = (\rho U, \rho C U, \rho U^2 + P, U(E + P), \rho \psi U)$  and suitable boundary conditions. A physically relevant entropy inequality must be added to select admissible shocks, which requires defining the specific entropy  $s(P, \rho, C, \psi)$ . The total energy is written in terms of the kinetic energy plus the internal energy  $\rho e$  which depends on density  $\rho$  and pressure  $P$ , but may also depend on concentration  $C$  and colour function  $\psi$ . Thus total energy is  $E = \rho U^2/2 + \rho e$  where  $\rho e$  is a function of  $(P, \rho, C, \psi)$  and  $U$  denotes the velocity. We then introduce classes  $T_1$  and  $T_2$  which contain EOS which respectively take the form:

$$\begin{cases} \rho e = \phi_1(P, \rho, C, \psi) = \rho(a_1(P) + b_1(P)C + c_1(P)\psi) + d_1(P) \\ \rho e = \phi_2(P, C, \psi) = f_2(C, \psi)h_2(P) + g_2(C, \psi) \end{cases} \quad (2)$$

We recall here that both  $C, \psi$  are regular solutions of the first equation of (6). Any EOS may be decomposed in terms of contribution in  $T_1 \cup T_2$  and the remaining part if necessary:  $\rho e = \phi_1(P, \rho, C, \psi) + f_2(C, \psi)h_2(P) + g_2(C, \psi) + \phi_3(P, \rho, C, \psi)$ . For instance, the perfect gas EOS and the Tamman law belong to  $T_1$ , and the mixture of perfect gases and the stiffened gas EOS lie in  $T_2$  exactly. If the EOS lies in  $T_1$ , standard conservative Godunov scheme (or conservative approximate Godunov scheme VFRoe-ncv with above mentionned variable  $Y$ ) perfectly represents unsteady contact discontinuities on any mesh. This means that when using standard definition of the pressure on each cell  $p_i^n = P_i^n$  solution of  $e(P_i^n, \rho_i^n, C_i^n, \psi_i^n) = e_i^n$ , and standard notations for the time step  $\delta t$ , the mesh size  $h_i = x_{i+1/2} - x_{i-1/2}$ , denoting  $W(Y_{x_{i+1/2}}^*)$  the interface value predicted by the exact or approximate Godunov scheme, the mean value of conservative variable  $W$  over cell  $i$  at time  $k\delta t$ , namely  $W_i^k$ , is obtained through:

$$h_i(W_i^{n+1} - W_i^n) + \delta t(F(W(Y_{x_{i+1/2}}^*)) - F(W(Y_{x_{i-1/2}}^*))) = 0 \quad (3)$$

## 3. Modified form of approximate or exact Godunov schemes

We now present the modified version of the explicit scheme, setting  $\gamma = \rho c^2/P$  for any EOS. For any EOS which does not lie in  $T_1$ , setting  $g_0(C, \psi) = f_2(C, \psi)h_2(P_{\text{ref}}) + g_2(C, \psi)$ , enables us to define the explicit first order version of the modified explicit scheme which is:

$$h_i(W_i^{n+1} - W_i^n) + \delta t(F(W(Y_{x_{i+1/2}}^*)) - F(W(Y_{x_{i-1/2}}^*))) = 0 \quad (4a)$$

$$h_i((g_0)_i^{n+1} - (g_0)_i^n) + \delta t \hat{U}_i((g_0)_{x_{i+1/2}}^* - (g_0)_{x_{i-1/2}}^*) = 0 \quad (4b)$$

$$h_i((\phi_3)_i^{n+1} - (\phi_3)_i^n) + \delta t \widehat{U}_i((\phi_3)_{x_{i+1/2}}^* - (\phi_3)_{x_{i-1/2}}^*) + \delta t \widehat{H}_i((U)_{x_{i+1/2}}^* - (U)_{x_{i-1/2}}^*) = 0 \quad (4c)$$

$$2\widehat{U}_i = U_{x_{i+1/2}}^* + U_{x_{i-1/2}}^* \quad (4d)$$

$$2\widehat{H}_i = \left( \gamma P \frac{\partial \phi_3}{\partial P} + \rho \frac{\partial \phi_3}{\partial \rho} \right)_{x_{i-1/2}}^* + \left( \gamma P \frac{\partial \phi_3}{\partial P} + \rho \frac{\partial \phi_3}{\partial \rho} \right)_{x_{i+1/2}}^* \quad (4e)$$

Any quantity  $m_{j+1/2}^*$  on interface  $j + 1/2$  stands for  $m(Y_{j+1/2}^*)$ . The definition of the numerical flux is the following:  $\widehat{F}(W(Y^*)) = (\rho^*U^*, \rho^*U^*C^*, \rho^*U^*U^* + P^*, U^*(\rho^*U^*U^*/2 + P^* + (\rho e)^*), \rho^*U^*\psi^*)$ , where:  $(\rho e)^* = \phi_1(P^*, \rho^*, C^*, \psi^*) + f_2(C^*, \psi^*)h_2(P^*) + g_2(C^*, \psi^*) + \phi_3(P^*, \rho^*, C^*, \psi^*)$ . Both series  $(f_2)_i^k$  and  $(g_2)_i^k$  issue from computation of  $g_0$  setting  $h_2(P_{ref}) = 0$  and  $h_2(P_{ref}) = 1$  successively. The cell pressure used to compute the local Riemann problems at the beginning of the next time step, namely  $p_i^{n+1} = \widetilde{P}_i^{n+1}$ , is obtained by computing the solution  $\widetilde{P}_i^{n+1}$  of equation:

$$\rho_i^{n+1} e_i^{n+1} - ((g_2)_i^{n+1} + (\phi_3)_i^{n+1}) = \phi_1(\widetilde{P}_i^{n+1}, \rho_i^{n+1}, C_i^{n+1}, \psi_i^{n+1}) + (f_2)_i^{n+1} h_2(\widetilde{P}_i^{n+1}) \quad (5a)$$

$$\rho_i^{n+1} e_i^{n+1} = E_i^{n+1} - \frac{(Q_i^{n+1})^2}{2\rho_i^{n+1}} \quad (5b)$$

with given values  $E_i^{n+1}$ ,  $Q_i^{n+1}$ ,  $\rho_i^{n+1}$ ,  $C_i^{n+1}$ ,  $\psi_i^{n+1}$  provided by discrete conservative equations, and  $(f_2)_i^{n+1}$ ,  $(g_2)_i^{n+1}$ ,  $(\phi_3)_i^{n+1}$  provided by discrete non-conservative equations. The resulting value of cell pressure is used to initialize Riemann problems at each cell interface at the beginning of the following time step. Discrete equations (4b)–(4e) are associated with governing equations:

$$\frac{\partial g_0}{\partial t} + U \frac{\partial g_0}{\partial x} = 0 \quad \text{and} \quad \frac{\partial \phi_3}{\partial t} + U \frac{\partial \phi_3}{\partial x} + \left( \gamma P \frac{\partial \phi_3}{\partial P} + \rho \frac{\partial \phi_3}{\partial \rho} \right) \frac{\partial U}{\partial x} = 0 \quad (6)$$

The latter two provide *redundent* information for regular solutions. Note that, for Chemkin EOS or for some complex analytic laws, the CPU time required to compute  $\widetilde{P}_i^n$  is lower than the CPU time for  $P_i^n$ . Unsteady contact discontinuities are now perfectly represented on any mesh size since we have (see [13]):

PROPERTY. – For any EOS in  $T_1 \cup T_2 \cup T_3$ , and for given initial data in agreement with:  $U_k^n = U_0$  and  $p_k^n = P_0$  with  $k = i - 1, i, i + 1$ , the modified Godunov scheme (4) ensures that  $p_i^{n+1} = P_0$ , and  $U_i^{n+1} = U_0$ . This is still true when using the above mentioned approximate Godunov scheme with  $Y^t = (U, P, g(\rho, s), C, \psi)$ .

#### 4. Numerical results

We focus here on the behaviour of schemes when at least one shock wave occurs in the solution. Detailed investigation of rates of convergence of the basic approximate Godunov scheme is available in [4], when restricting to EOS in  $T_1$  such as perfect gas state law or Tamman EOS. In addition the rate of convergence of variables supported by the contact discontinuity such as the mean concentration is clearly 1/2 (see [4]). Numerical tests have been obtained using  $Y^t = (U, P, \rho, C, \psi)$ .

##### 4.1. EOS in the second class

Results below are associated with the stiffened gas EOS or equivalently with a mixture of perfect gases (see [6,7] for instance). Decomposition gives:  $\rho e = \phi_2(P, C, \psi) = f_2(C, \psi)P + g_2(C, \psi)$  with  $f_2(C, \psi) = 1/(\gamma(\psi) - 1)$ , and  $g_2(C, \psi) = P_{inf}(\psi)/(\gamma(\psi) - 1)$ . Recall that  $\phi_1(P, \rho, C, \psi) = 0$ ,  $\phi_3(P, \rho, C, \psi) = 0$  here. Fig. 1 represents a shock tube, computed by the VFRoe-ncv  $(\rho, U, P, C)$  scheme and its hybrid modification. Fig. 2 refers to the measure of the  $L^1$  norm of the error when computing a pure 3-shock wave followed by a moving contact discontinuity with the hybrid scheme (the rate of convergence is close to 1/2 (respectively 1) for  $\rho$  (resp.  $U, P$ )) and with the basic VFRoe-ncv scheme (the rate of convergence is close to 1/2 for  $\rho, U, P$ ). Meshes contain from 100 to 160000 cells.

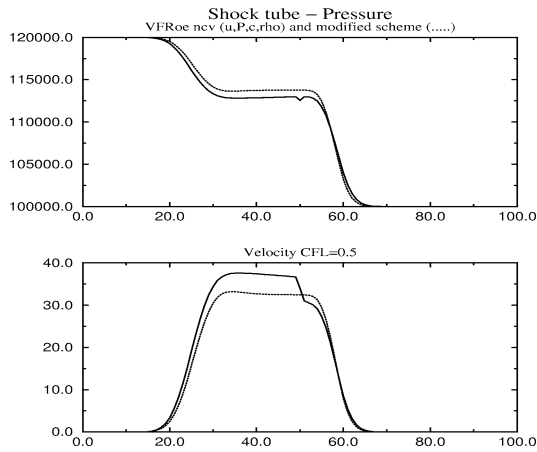


**Figure 1.** Shock tube – stiffened gas EOS – coarse mesh.

**Figure 1.** Tube à choc – stiffened gas EOS – maillage grossier.

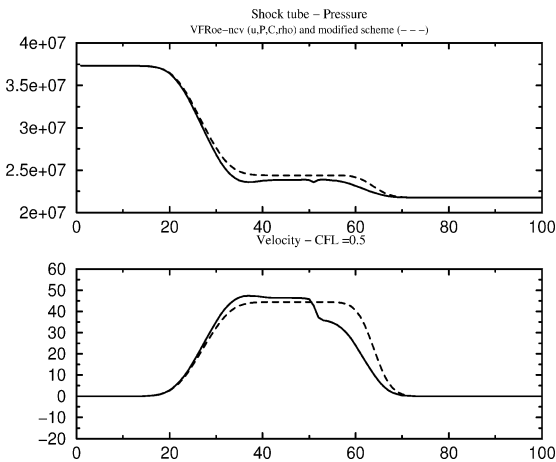


**Figure 3.** Shock tube – Van der Waals EOS – coarse mesh.

**Figure 3.** Tube à choc – Van der Waals EOS – maillage grossier.

#### 4.2. EOS in the third class

We turn now to Van der Waals EOS (see [8]). Decomposition of EOS can be written:  $\rho e = \phi_1(P, \rho, C, \psi) + \phi_3(P, \rho, C, \psi)$ ,  $\phi_2(P, C, \psi) = 0$ , where  $b_1(P) = c_1(P) = 0$ ,  $d_1(P) = P/(\gamma - 1)$ ,  $a_1(P) = -bP/(\gamma - 1)$ ,  $\phi_3(P, \rho, C, \psi) = a\rho^2(-b\rho + 2 - \gamma)(\gamma - 1)^{-1}$ . Fig. 3 provides computational results obtained with both schemes, when approximating shock tube apparatus. Fig. 4 refers to the  $L^1$  error norm when computing a 3 shock wave with the hybrid scheme and the basic conservative scheme (for which the rate of convergence is still 1/2 for  $\rho, U, P$ ). Meshes contain from 100 to 20000 cells.

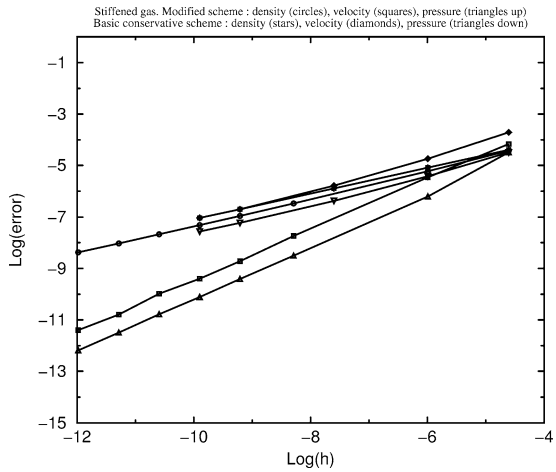


**Figure 2.** Pure unsteady 3-shock – stiffened gas EOS –  $L^1$  error norm.

**Figure 2.** 3-choc pur instationnaire – stiffened gas EOS – erreur en norme  $L^1$ .

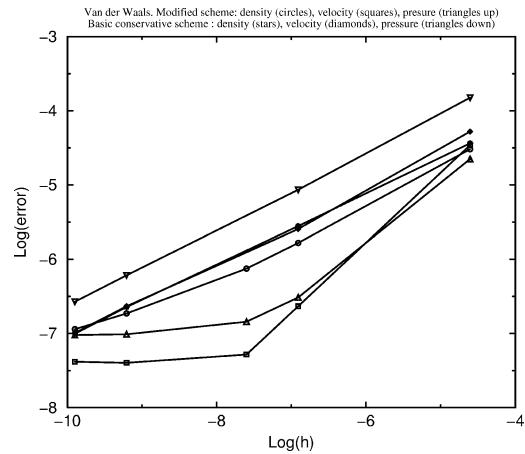


**Figure 4.** Pure unsteady 3-shock – Van der Waals EOS –  $L^1$  error norm.

**Figure 4.** 3-choc pur instationnaire – Van der Waals EOS – erreur en norme  $L^1$ .

## 5. Conclusion

The hybrid method enables to increase accuracy of computations on coarse meshes, and also to get rid of some oscillations in some cases. It has been applied in a very wide class of numerical tests including double shock waves, double rarefaction waves, combination of contact discontinuity with ghost 1 wave and 3 shock wave, and many EOS including those discussed herein, Chemkin database and tabulated EOS. This has been achieved using meshes with 100 up to 160000 nodes. The influence of the decomposition is examined in [13] which shows that a ‘correct’ decomposition should be preferred to a ‘wrong’ decomposition (for instance by enforcing the perfect gas EOS in  $T_3$  instead of  $T_1$ ), as expected, and in relation to the work in [9]. This nonetheless appears when using fine meshes which are far beyond the reach of current computer facilities for industrial purposes (this would concern meshes with more than  $10^{12}$  nodes in a three dimensional framework). The modified scheme is thus useful: for given – coarse – mesh size it is in practice less time consuming (at least when dealing with complex analytic EOS) and more accurate than the initial fully conservative scheme. Higher order schemes may be derived using standard MUSCL approach. A blend scheme also seems appealing for industrial purposes, in order to benefit from properties of modified and initial – fully conservative – schemes (see [13]).

## References

- [1] S.K. Godunov, A difference method for numerical calculation of discontinuous equations of hydrodynamics, *Sbornik* (1959) 271–300 (in Russian).
- [2] E. Godlewski, P.A. Raviart, *Numerical Approximation of Hyperbolic Systems of Conservation Laws*, Appl. Math. Series, Vol. 118, Springer-Verlag, 1996.
- [3] T. Buffard, T. Gallouët, J.M. Hérard, A sequel to a rough Godunov scheme. Application to real gas flows, *Comput. Fluids* 29 (7) (2000) 813–847.
- [4] T. Gallouët, J.M. Hérard, N. Seguin, Some recent Finite Volume schemes to compute Euler equations using real gas EOS, Preprint LATP 00-021, 2000, *Int. J. Numer. Methods Fluids*, to appear.
- [5] S. Karni, Multicomponent flow calculations by a consistent primitive algorithm, *J. Comput. Phys.* 112 (1994) 31–43.
- [6] R. Abgrall, How to prevent pressure oscillations in multicomponent flow calculations: a quasi conservative approach, *J. Comput. Phys.* 125 (1995) 150–160.
- [7] R. Saurel, R. Abgrall, A simple method for compressible multifluid flows, *SIAM J. Sci. Comput.* 21 (3) (1999) 1115–1145.
- [8] K.M. Shyue, A fluid mixture type algorithm for compressible multicomponent flow with Van der Waals equation of state, *J. Comput. Phys.* 156 (1999) 43–88.
- [9] X. Hou, P.G. Le Floch, Why nonconservative schemes converge to wrong solutions, *Math. Comput.* 62 (1995) 497–530.
- [10] A. Letellier, A. Forestier, Le problème de Riemann en fluide quelconque, CEA-DMT Report 93/451, 1993.
- [11] R. Kee, J. Miller, T. Jefferson, Chemkin: a general purpose, problem independent transportable fortran chemical kinetics code package, SAND Report 80-8003, Sandia National Laboratories.
- [12] P. Rasclé, O. Morvant, Interface utilisateur de Thetis – THERmodynamique en Tables d’Interpolations, EDF-DER Report HT-13/95021B, 1995.
- [13] T. Gallouët, J.M. Hérard, N. Seguin, Hybrid schemes to compute contact discontinuities in Euler systems, EDF report HI-81/01/011/A, 2001.
- [14] G. Allaire, S. Clerc, S. Kokh, A five equation model for the numerical solution of interfaces in two phase flows, *C. R. Acad. Sci. Paris, Série I* 331 (2000) 1017–1022.